2019 International Symposium on Lightning Protection (XV SIPDA), São Paulo, Brazil, 30th September – 4th October 2019.

Simplified 3-D Modeling of Reinforced Concrete for the Calculation of Transient Electromagnetic Fields inside a Building Struck by Lightning

S. Naranjo-Villamil, J.Gazave
Laboratoire des Matériels Electriques
Electricité de France
Moret-sur-Loing, France

C.Guiffaut, A. Reineix
CEM et Diffraction
Institut de recherché XLIM
Limoges, France

***Abstract*—Although the impact of the lightning electromagnetic pulse can be well approximated by using full-wave methods, generally the simulations demand a long computation time and large memory requirements, due to the number of elements that have to be included in the model of the electromagnetic environment. In this paper, we present an optimization technique to simplify the 3-D representation of the reinforcement, in case of a direct strike. By reducing the multi-layered steel grid into a single-layered grid, a solution for all points in the environment can still be obtained, using less computational resources.**

Keywords— Reinforced concrete, electromagnetic field, lightning, Kriging.

I. INTRODUCTION

Reinforced concrete usage as a part of the lightning protection system (LPS) has increasingly gained popularity. The layers of steel grid embedded in concrete walls work as a natural down-conductor to the ground when a building is struck by lightning, reducing the impact of the lightning electromagnetic pulse (LEMP). Yet, the electromagnetic field produced by the flow of the current through the rebars during a direct strike, can cause malfunctioning of sensitive electronic equipment and electrical surges, leading to physical damage [6]. Therefore, to appropriately design the LPS and select a surge protection device, the transient electromagnetic field inside the building needs to be evaluated.

Numerous analysis of the shielding characteristics of reinforced concrete walls have been conducted [1]-[5]. Numerical and experimental results of research carried out to study the effect of the LEMP in reinforced concrete structures can be found in [6]-[10]. Generally, two main types of simulation methods are employed to calculate the electromagnetic fields inside buildings: the Transmission Line theory method, which has been widely used due to its simplicity and the full-wave methods. In terms of precision, using a full-wave approach allows one to obtain more accurate results because it fully accounts the coupling between the wires and the physical characteristics of each component of the model. However, when the problem is geometrically complex, which is usually the case for a full-scale reinforced concrete building, solving Maxwell's equations for a complete electromagnetic environment requires a high amount of computational resources.

Aiming to find a compromise between accuracy and practicality, we present a technique to simplify the 3-D model of multi-layer grid-like shields. Initially, a reduced representation of reinforced concrete walls is proposed to evaluate its shielding effectiveness. In the reduced representation, the main features of any reinforcing grid can be considered and the shield characterized, based on the current and the magnetic field produced when a voltage source is connected to the rebars.

Applying the Design of Experiments (DoE) theory [11] and machine learning algorithms, several regression models are obtained from the reduced representation of single-layered reinforcing grids. In accordance with the normalized root-mean-square error (NRMSE) estimated for each model, the Kriging interpolation method is chosen and two meta-models are trained: the first for the current and the second for the magnetic field. As an example, these meta-models are then used to find the characteristics of the equivalent shield of a multi-layered grid. Finally, the technique is validated by comparing the calculated electromagnetic fields inside a 15-meters-tall building and the same structure with its equivalent reinforcement. The simulations are carried out in TEMSI-FD, a solver based on the finite-difference time-domain method (FDTD) [12].

II. REPRESENTATION OF THE REINFORCEMENT

Reinforced concrete buildings are commonly modeled using the thin-wire approach in which the rebars are represented by a junction of lossy thin wires. In the reinforcement, the number of layers, the mesh size, the radius of the rebars and the distance between the hoops vary depending on the case. The effect of these variations on the shielding can be studied using a reduced representation of the reinforcing grid.

We propose an 8×8 m^2 grid made of thin wires [13] with an electrical conductivity of 8.33×10^3 S/m in a perfectly conducting metallic enclosure of $10 \times 10 \times 3$ m^3. The first layer of the grid is connected, from one side to the enclosure, and

from the other side to a perfect voltage source which is connected to the enclosure. The connecting wires are perfectly conducting with a radius of 2.5 cm. The voltage is a Gaussian function with a maximum value of 100V, an attenuation of 10^6 in $t = 0$ s and of 10 in $f_{max} = 1$MHz. To characterize the shield we consider two variables of interest: the current traveling through the grid and the magnetic field it induces. The current is calculated in the wire directly attached to the enclosure and an approximation of the magnetic field is obtained from the average of the magnetic fields in a 2×2 m^2 surface, located in the center of the enclosure, one meter away from the first layer of the grid. Note that the conductivity of the steel has been divided by 10^3. This change, as well as using a metallic enclosure, is made to reduce the calculation time and with the purpose of minimizing the effects of the connecting wires in the results.

To illustrate, Fig. 1 shows the representation of a double-layered grid adapted from [10]. The grid has 0.3×0.3 m^2 meshes and its rebars have a radius of 1.4 mm. The distance between the layers is 0.3 m and they are connected every 0.9 m. To keep the grid size constant in all the reduced representations, the meshes of the last row and the last column are not necessarily squared, they can also be rectangular. This approximation simulates a similar situation which occurs when the building dimensions are not a multiple of the mesh size.

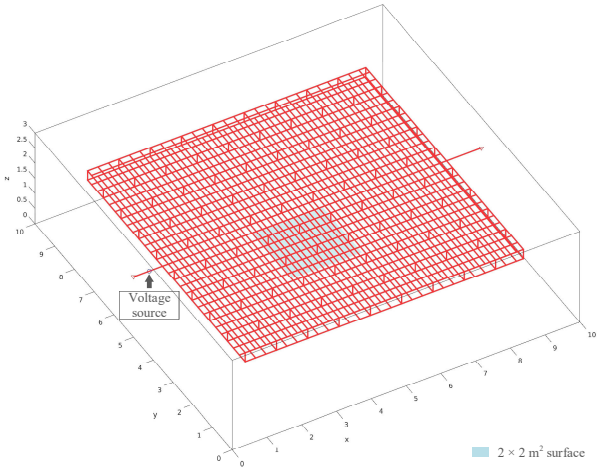

Fig. 1. Reduced representation of a double-layered reinforcing grid.

TABLE I. LEVELS FOR THE SINGLE-LAYERED REINFORCED GRID EXPERIMENT.

Factors	Levels									
	1	*2*	*3*	*4*	*5*	*6*	*7*	*8*	*9*	*10*
Radius [mm]	0.5	1	1.5	2	2.5	3	3.5	4	4.5	5
Mesh size [m]	0.1	0.2	0.3	0.4	0.5	0.6	0.7	0.8	0.9	1

III. META-MODEL OF SINGLE-LAYERED GRIDS

A. *Factorial design*

Considering the reduced representation of a single-layered reinforcing grid as an experiment with two inputs: the radius of the rebars and the mesh size, and two outputs: the current and the magnetic field, as defined in the previous section, to study the effects of the variation of the inputs in the responses, 100 calculations are executed based on a 10^2 factorial plan where all the interactions between the two factors at 10 levels are taken into account. The levels are given in Table I.

For the simulations, the size of the FDTD cells is set to 0.1 m and the observation time to 20μs. The results are shown in Fig. 2 and Fig. 3. It can be seen that both the current and the magnetic field reach higher levels when the radius increases and the mesh size decreases. This behavior can be easily modeled using Analysis of Variance [11] when considering only the peak-values. However, we decided to include the time as an input to keep information about the attenuation, which could be as useful as the peak to fit the expression of the models obtained for single-layered grids, to the response curve of a multi-layered grid. Consequently, 65 uniformly spaced samples of the time responses are taken to build a dataset to train two regression models, one for each output.

Using Matlab, five regression model types are tested: Linear Regression, Regression Trees, Support Vector Machines (SVM), Gaussian Process Regression (GPR) and Ensemble of Trees. Table II shows the best models based on the NRMSE, estimated by applying a 10-fold cross validation. Since the GPR algorithms, also known as Kriging, seem to make the best predictions, we focused on obtaining Kriging meta-models.

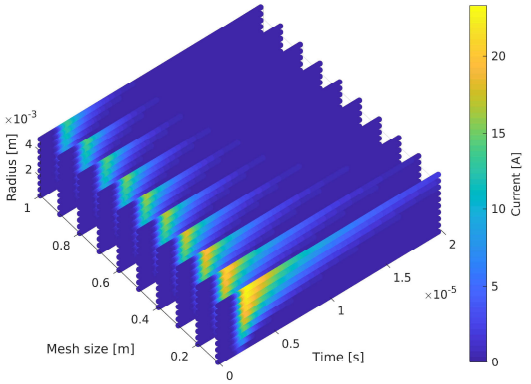

Fig. 2. Current traveling through the grid.

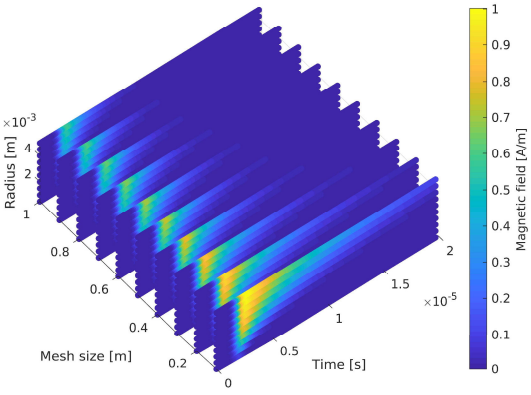

Fig. 3. Magnetic field induced.

TABLE II. BEST ADJUSTED MODELS BASED ON THE NRMSE.

	Model	*NRMSE*
Current	GPR with Rational Quadratic kernel	2.1795×10^{-4}
	GPR with Matern 5/2 kernel	2.8099×10^{-4}
	GPR with Exponential kernel	3.0606×10^{-3}
	Fine Tree (minimum leaf size = 4)	1.7645×10^{-2}
	Boosted Trees (30 learners and minimum leaf size = 8)	3.0460×10^{-2}
Magnetic field	GPR with Rational Quadratic kernel	4.0173×10^{-4}
	GPR with Matern 5/2 kernel	4.7341×10^{-4}
	GPR with Exponential kernel	3.1276×10^{-3}
	GPR with Squared Exponential Kernel	1.5195×10^{-2}
	Fine Tree (minimum leaf size = 4)	1.8348×10^{-2}

TABLE III. PARAMETERS OF THE SELECTED KRIGING META-MODELS.

Parameter	*Model of the current*	*Model of the magnetic field*
β_1	36.1010	1.3368
σ^2	259.2452	0.3184
θ	[8.5335 7.7402 1.2628]	[7.2819 6.9235 1.1565]
LOO	4.8310×10^{-6}	4.9759×10^{-6}

B. Kriging

Given a dataset $\{(x_i, y_i);\ i = 1,2,\dots,n\}$ where $x_i \in \mathbb{R}^s$ and $y_i \in \mathbb{R}$, a linear regression model would be of the form

$$u(x) = \beta^T x,\ y = u(x) + \varepsilon, \tag{1}$$

where x is the input vector, y is the output vector, β is the vector of regression parameters and ε is the vector of residuals. To implement a different kind of regression, the input vector can be projected into an N dimensional feature space using a set of mapping functions. The model becomes then

$$u(x) = \beta^T F, y = u(x) + \varepsilon, \tag{2}$$

where $F = [f_k(x_i)]$ represent the user-selected basis functions that transform the original vector, β is the vector of the functions coefficients, $u(x)$ is a deterministic function approximating the mean value of the output and ε is the error.

Kriging is a popular interpolation method which assumes that the model output is a realization of a stochastic process by considering the error ε as a zero mean, stationary Gaussian Process (GP)

$$u(x) = \beta^T F, y = u(x) + \varepsilon(x), \tag{3}$$

$$\varepsilon(x) \sim GP\big(0, k(x,x')\big), k(x,x') = \sigma^2 R(x,x';\theta), \tag{4}$$

where the mean value of the output $u(x)$ is called the Kriging trend, σ^2 is the process variance, $R(x,x';\theta)$ is the kernel function describing the correlation between two samples and θ its hyperparameters.

A GP is defined as a collection of random variables such that the examination of a larger set of variables does not change the distribution of a smaller set [14]. Therefore, a Kriging meta-model predicts the responses assuming that the vector formed by the true responses and the predictions has a joint Gaussian distribution [15], and consequently the parameters β and σ^2 can derived by maximizing the likelihood function

$$L(y|\beta,\sigma^2,\theta) = \frac{\det(R)^{-1/2}}{(2\pi\sigma^2)^{N/2}} exp\left[-\frac{1}{2\sigma^2}(y - F\beta)^T R^{-1}(y - F\beta)\right], \tag{5}$$

where R is the correlation matrix

$$R_{ij} = R\big(x_i, x_j; \theta\big), i, j = 1,2,\dots,N. \tag{6}$$

There are various types of Kriging, depending on the trend that is employed. We decided to use ordinary Kriging, where the trend has a constant value

$$u(x) = \beta^T F = \beta_1 f_1(x) = \beta_1, \tag{7}$$

A kernel is not initially selected, thus different Kriging predictors are obtained and compared using UQLab [16]. Assuming that all the inputs have a uniform distribution, the best models, based on the calculated leave-one-error (LOO), are found with the Matern 5/2 kernel. To estimate the parameters of the models, the optimization problem which results from the evaluation of the maximum likelihood, as a function of θ, needs to be solved. Therefore, a Hybrid Genetic Algorithm (HGA) is implemented with a convergence tolerance of 10^{-10} and the maximum number of generations equals to 500. The results are presented in Table III.

C. Model fitting criteria

Going back to the purpose of the technique introduced in this paper, the idea is to determine the characteristics of an equivalent single-layered grid, by approximating the input vector to be used in the Kriging meta-models, in order to find the same current and the same magnetic field obtained in the reduced representation of a multi-layered grid.

To approximate the components of the input vector, which correspond to the radius of the rebar and the mesh size of an equivalent single-layered grid, they are considered as the unknown parameters of two non-linear models. These models are then fitted to the response curves of the reduced representation of a multi-layered grid using least squares. For the fitting, the tolerance on the model value and on the coefficients values is set to 10^{-10}. The procedure is summarized in Fig. 4.

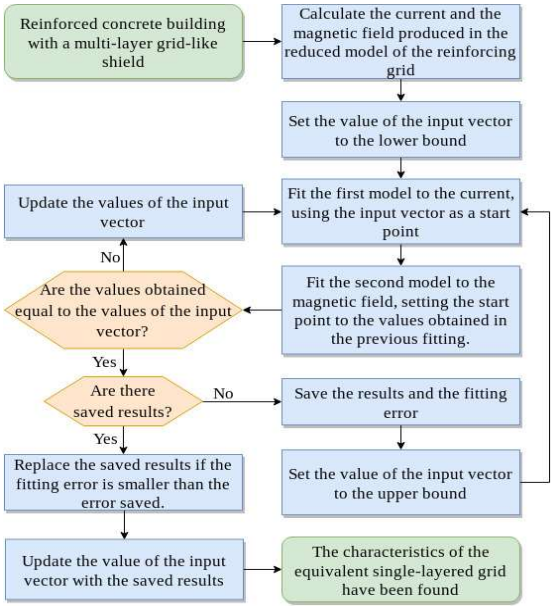

Fig. 4. Flowchart of the fitting algorithm.

As an example, consider the shield described in section II and its reduced representation shown in Fig.1. Implementing the fitting algorithm, the lowest error is found starting from the lower bound of the models and the equivalent grid obtained has rebars with a radius of 1.13 mm and a mesh size of 0.1026 m. The first model is fitted to the current with a NRMSE of 0.0014 and the second model is fitted to the magnetic field with a NRMSE of 0.0039. The results are shown in Fig. 5 and Fig. 6.

The components of the input vector could be approximated fitting only one model to one response curve, as well as starting the optimization from a random point. However, the solution may not always be unique and in some cases it may not be accurate. To address this problem, the algorithm compares the values obtained with two independent models and the error when starting from two different points. If there were two solutions, they would be found starting from the lower and the upper bounds.

We observed that when starting the fitting from the lower bound, the simplification of the multi-layered grid is usually compensated by a smaller mesh size, while starting from the upper bound it is compensated by a bigger radius. Rarely the second approach is a better fit and the algorithm manages to find an equivalent grid without drastically reducing the mesh size. When it comes to estimate the error of the electromagnetic fields produced by the equivalent grid in a full-scale building, the first approach always gives better results.

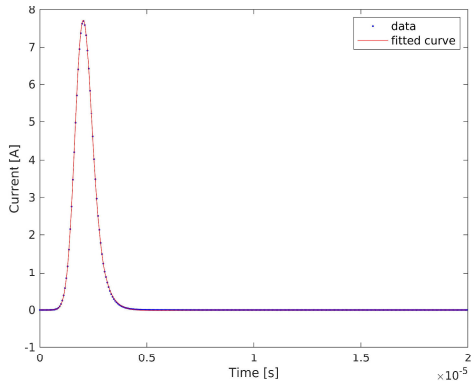

Fig. 5. Fitted curve for the current obtained from the reduced representation of a double-layered grid.

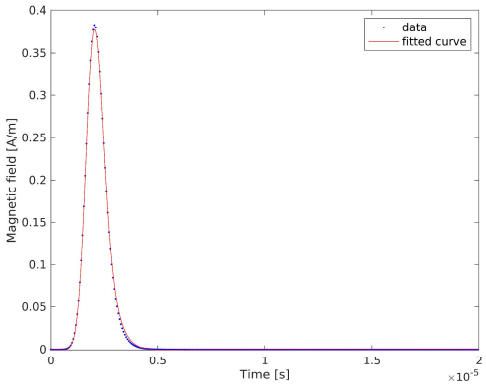

Fig. 6. Fitted curve for the magnetic field obtained from the reduced representation of a double-layered grid.

IV. CASE STUDY

To verify that an equivalent grid found using the algorithm has the same shielding effectiveness as the multi-layered grid in a full-scale building struck by lightning, the electromagnetic fields produced by a direct strike are computed in a single-story 15-meters-tall structure, with a horizontal cross-sectional area of 10×10 m^2. The external walls, the roof and the foundation of the structure are made up of the double-layered reinforcing grid used in the example, embedded in 0.4 m of concrete, which is modeled as a lossy dielectric material with a conductivity of 0.0052 S/m and a relative permittivity of 8.6. The foundation is buried one meter away from the surface. No internal walls, columns or beams are considered. The conductivity of the rebars is set to 8.33×10^6 S/m and the size of the FDTD cells to 5 cm.

The lightning channel is represented applying the transmission line (TL) model with the current of a negative subsequent stroke, protection level I, as defined in the standard IEC62305. Its attachment point is chosen to be in the corner of the roof as shown in Fig.7.

The fields are calculated in 12 horizontal surfaces distanced one meter away from each other and from the foundation. The magnitudes decrease with the increase of the distance between the attachment point and the observation point, but they start increasing again close to the foundation. The highest values are obtained in surface 12, which is just below roof. The maximum of the electric and the magnetic fields are shown in Fig. 8 and Fig. 9.

Executing the same computation with the equivalent grid instead of the double-layer shield, an identical distribution of the field is obtained, besides a slight difference in about 5 centimeters next to the walls. This difference is due to the fact that the equivalent grid is placed where the outer layer of the original grid was, thus the inhomogeneity in the field created by the rebars that were near the interior of the building is no longer visible. The choice of the position of the equivalent grid inside the walls is based on the injected current waveform and the distribution of the currents in the reinforcement. In multi-layer shields, the faster the current rises, the more the current is displaced to the outer grid [17].

The relative error in magnitude is 5% in average, yet, a higher error can be found close to the walls and to the edges, since the highest currents flow through the corner wires. In these points the values change very fast, therefore an improvement can be expected if the cell size is reduced. . The fields in surface 12 are shown in Fig. 10 and Fig. 11. The relative error is shown in Fig. 12 and Fig. 13.

The results confirm that a multi-layered grid can be replaced by an equivalent single-layered grid found using the technique developed, as long as an average value of the fields next to the walls is accepted. If it is essential to reproduce the inhomogeneity created by the rebars, the equivalent grid can be placed where the inner grid used to be, but it will lead to less accurate results in the rest of the surface.

The question regarding the amount of computational resources that can be reduced still remains. To obtain both the impedance and the shielding effectiveness of the original

reinforcement with an equivalent grid, the mesh size must be reduced. In that case, the only gain that could be achieved would be in terms of memory. Expanding the factorial design and adding the conductivity of the rebars as an input, we can find other solutions in which the mesh size is bigger than the original, assuring that the characteristics of the equivalent grid are convenient and the computation time can be reduced. Yet, a choice has to be made between approximating the complex impedance and approximating the electromagnetic fields. We are considering other techniques and adding constraints in the optimization process to improve the fitting algorithm.

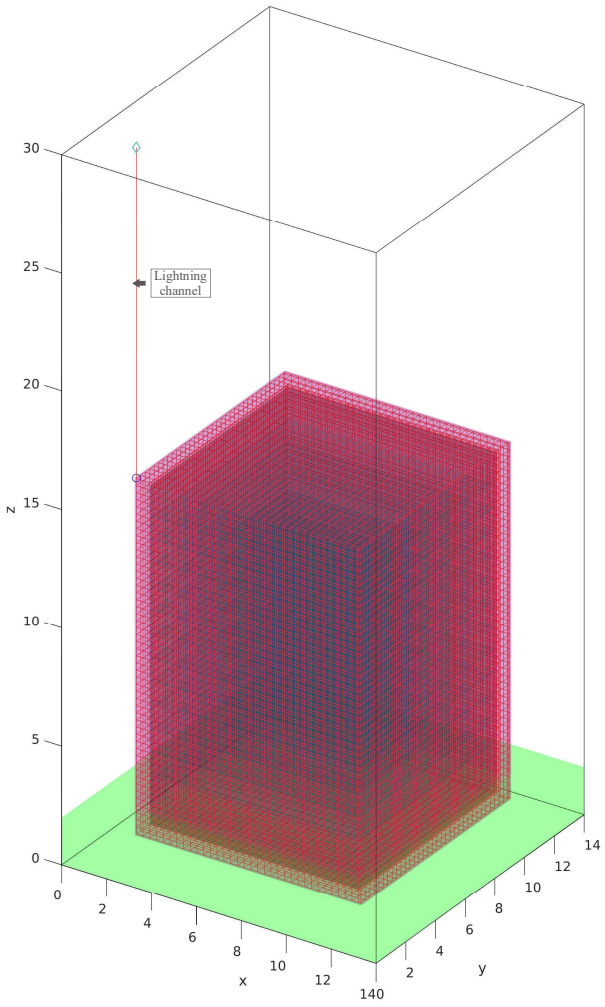

Fig. 7. Calculation model of a 15-meters-tall building with a double-layer grid-like shield, directly struck by lightning at point (2,2,16).

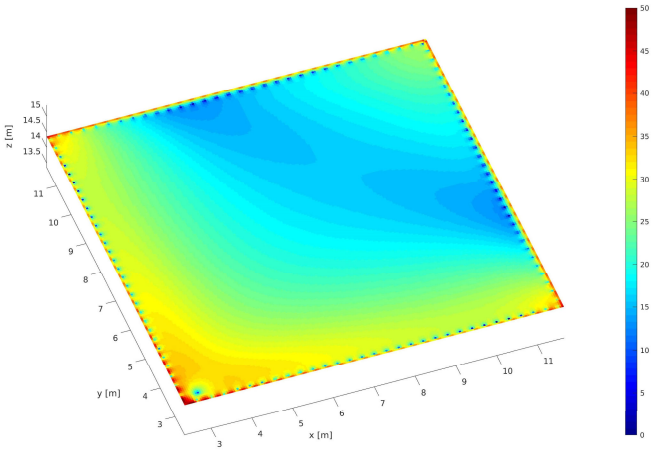

Fig. 8. Maximum magnetic field (dBA/m) in surface 12 with the original reinforcing grid.

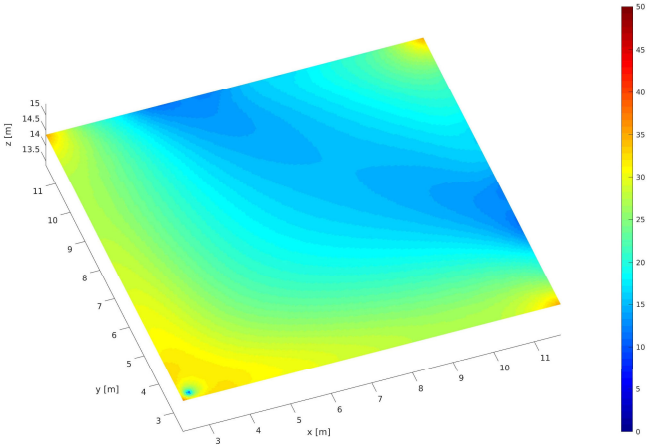

Fig. 9. Maximum magnetic field (dBA/m) in surface 12 with the equivalent reinforcing grid.

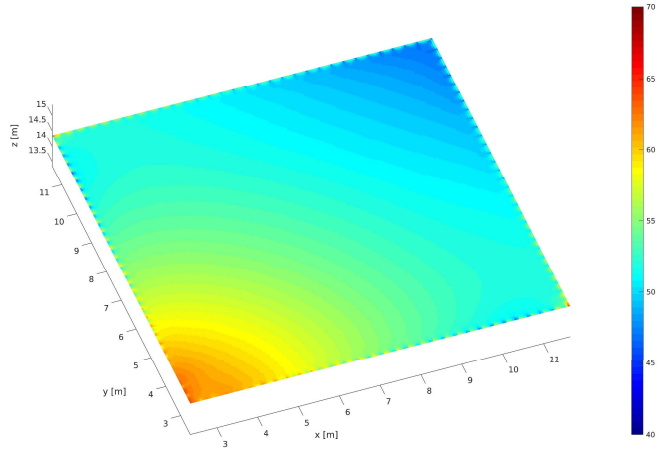

Fig. 10. Maximum electric field (dBV/m) in surface 12 with the original reinforcing grid.

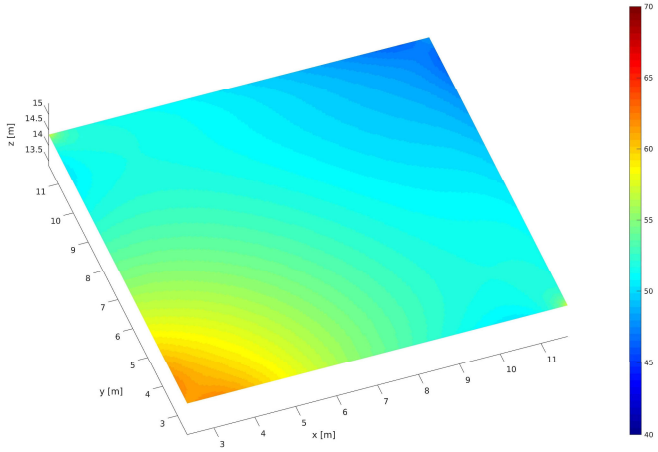

Fig. 11. Maximum electric field (dBV/m) in surface 12 with the equivalent reinforcing grid.

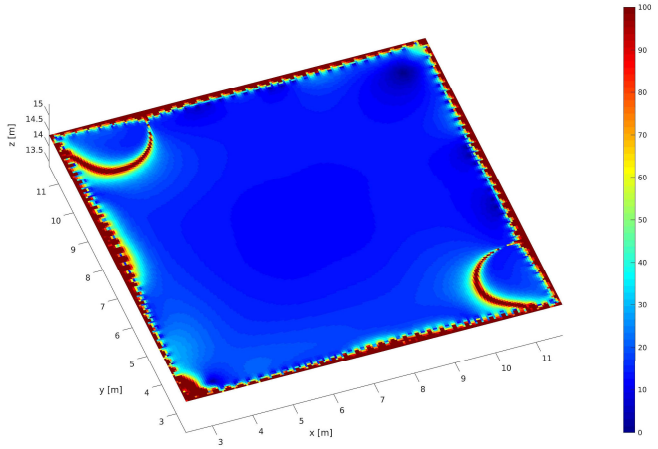

Fig. 12. Relative error (%) in the magnetic field in suface 12.

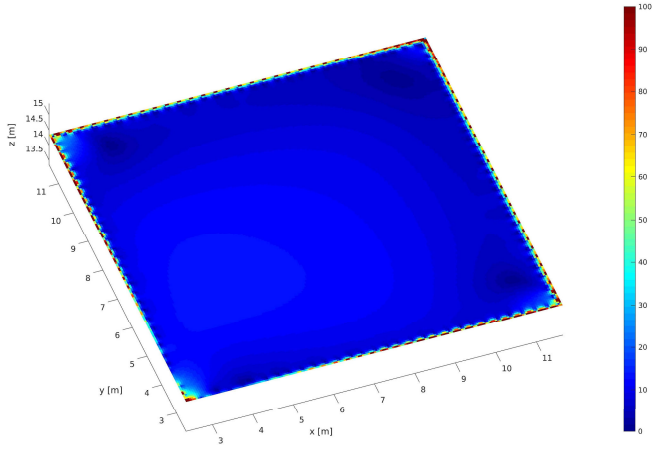

Fig. 13. Relative error (%) in the electric field in suface 12.

V. CONCLUSION

The technique introduced allows one to find a single-layered reinforced grid that could replace the multi-layer grid-like shield of a reinforced concrete building, when computing the electromagnetic fields produced by a direct strike inside the structure. This simplification could be useful in some cases to reduce the computational resources required to simulate a complete electromagnetic environment, using a solver based on a full-wave method. The results presented confirm the applicability of the technique, however, it is necessary to study a wide variety of buildings in order to determine its accuracy and robustness. The conductivity of the rebars could be added as an input of the models in order to find equivalent grids with a bigger mesh size, but in this case, the conditions under which modeling a structure with an equivalent reinforcement is advantageous would have to be evaluated.

REFERENCES

[1] E. Richalot, M. Bonilla, Man-Fai Wong, V. Fouad-Hanna, H. Baudrand, and J. Wiart, "Electromagnetic propagation into reinforced-concrete walls," *IEEE Transactions on Microwave Theory and Techniques*, vol. 48, no. 3, pp. 357–366, Mar. 2000.

[2] D. Pena, R. Feick, H. D. Hristov, and W. Grote, "Measurement and modeling of propagation losses in brick and concrete walls for the 900-MHz band," *IEEE Transactions on Antennas and Propagation*, vol. 51, no. 1, pp. 31–39, Jan. 2003.

[3] K. F. Casey, "Electromagnetic shielding behavior of wire-mesh screens," *IEEE Transactions on Electromagnetic Compatibility*, vol. 30, no. 3, pp. 298–306, Aug. 1988.

[4] R. A. Dalke, C. L. Holloway, P. McKenna, M. Johansson, and A. S. Ali, "Effects of reinforced concrete structures on RF communications," *IEEE Transactions on Electromagnetic Compatibility*, vol. 42, no. 4, pp. 486–496, Nov. 2000.

[5] S.-Y. Hyun *et al.*, "Analysis of Shielding Effectiveness of Reinforced Concrete Against High-Altitude Electromagnetic Pulse," *IEEE Transactions on Electromagnetic Compatibility*, vol. 56, no. 6, pp. 1488–1496, Dec. 2014.

[6] I. A. Metwally and F. H. Heidler, "Reduction of Lightning-Induced Magnetic Fields and Voltages Inside Struck Double-Layer Grid-Like Shields," *IEEE Transactions on Electromagnetic Compatibility*, vol. 50, no. 4, pp. 905–912, Nov. 2008.

[7] A. Tatematsu, F. Rachidi, and M. Rubinstein, "Analysis of Electromagnetic Fields Inside a Reinforced Concrete Building With Layered Reinforcing Bar due to Direct and Indirect Lightning Strikes Using the FDTD Method," *IEEE Transactions on Electromagnetic Compatibility*, vol. 57, no. 3, pp. 405–417, Jun. 2015.

[8] I. A. Metwally, W. J. Zischank, and F. H. Heidler, "Measurement of Magnetic Fields Inside Single- and Double-Layer Reinforced Concrete Buildings During Simulated Lightning Currents," *IEEE Transactions on Electromagnetic Compatibility*, vol. 46, no. 2, pp. 208–221, May 2004.

[9] C. Miry, E. Amador, P. Duquerroy, E. Bachelier, D. Prost, and F. Issac, "Evaluation of lightning induced magnetic fields inside reinforced concrete buildings," in *2013 International Symposium on Lightning Protection (XII SIPDA)*, Belo Horizonte, 2013, pp. 145–150.

[10] T. Maksimowicz and K. Aniserowicz, "Investigation of Models of Grid-Like Shields Subjected to Lightning Electromagnetic Field: Experiments in the Frequency Domain," *IEEE Transactions on Electromagnetic Compatibility*, vol. 54, no. 4, pp. 826–836, Aug. 2012.

[11] D. C. Montgomery, *Design and Analysis of Experiments*, 6th ed. New York: John Wiley & Sons, 2005.

[12] XLIM Institute, “TEMSI-FD: Time Electromagnetic Simulator - Finite Difference Time Domain,” Limoges, France, Apr. 2015.

[13] C. Guiffaut, A. Reineix and B. Pecqueux, “New oblique thin wire formalism in the FDTD method with multiwire junction,” *IEEE Trans. Antennas and Propag.*, vol. 60, no. 8, pp. 1458–1466, March 2012.

[14] C. E. Rasmussen and C. K. I. Williams, *Gaussian Processes for Machine Learning*. MIT Press, 2006.

[15] C. Lataniotis, S. Marelli and B. Sudret, UQLAB user manual – Kriging (Gaussian process modelling), Report UQLab-V1.2-105, Chair of Risk, Safety & Uncertainty Quantification, ETH Zurich, 2019.

[16] S. Marelli, and B. Sudret, UQLab: A framework for uncertainty quantification in Matlab, Proc. 2nd Int. Conf. on Vulnerability, Risk Analysis and Management (ICVRAM2014), Liverpool, United Kingdom, 2014, 2554-2563

[17] W. Zischank et al., “Laboratory simulation of direct lightning strokes to a modeled building: measurements of magnetic fields and induced voltages,” *Journal of Electrostatics*, vol. 60, pp. 223–232, 2014.